Available online at www.sciencedirect.com
ScienceDirect
Ceramics International 36 (2010) 2039–2045
CERAMICS INTERNATIONAL
www.elsevier.com/locate/ceramint

Effects of carbothermal reduction on the thermal and electrical conductivities of aluminum nitride ceramics

Hui-sik Kim [a,b], Jung-min Chae [a], Yoon-suk Oh [a], Hyung-tae Kim [a], Kwang-bo Shim [b], Sung-min Lee [a,*]

[a] Engineering Ceramics Department, Korea Institute of Ceramic Engineering and Technology (Icheon), Gyeonggi-do 467-843, Republic of Korea
[b] Department of Ceramic Engineering, CPRC, Hanyang University, Seoul 133-791, Republic of Korea

Received 27 January 2010; received in revised form 9 February 2010; accepted 27 April 2010
Available online 18 June 2010

Abstract

This study attempts to control the oxygen content by adding various amounts of yttria sintering additives or by introducing an *in situ* carbothermal reduction using a carbon addition during the Power processing step. While both yttria and the carbon addition increased the thermal conductivity and electrical resistivity, carbon addition was more effective in increasing the DC volume resistivity for specimens that had 3 or 5 wt% Y_2O_3. Among several elements of the electrical conductivities of the grains and grain boundaries, the conductivity of the grains appeared to be more relevant to the thermal conductivities of AlN ceramics. In addition, yttrium enrichment was observed in the grain boundary region. We also found that an *in situ* carbothermal reduction resulted in a small amount of yttrium-aluminate second phases, which are beneficial to the plasma resistance of the AlN ceramics.

Keywords: Thermal conductivity; Electrical conductivity; Aluminum nitride; Carbothermal reduction

1. Introduction

Aluminum nitride, whose theoretical thermal conductivity is 320 W/mK, is a new type of material for electrostatic chucks and heaters in the semiconductor industry. In such applications, the electrical conductivity of the ceramics must be well-optimized, in addition to a high thermal conductivity, as the working mechanism depends on the electrical properties under a high electric field [1–5].

Oxygen impurity has been studied widely to understand the thermal and electrical properties of AlN ceramics [6–18]. An oxygen content of approximately 0.8 wt%, inherent to commercial AlN powder, is mostly removed from the AlN grains through forming a grain boundary second phase with sintering additives such as Y_2O_3 and CaO [8–10]. As described by Slack et al. [11], the remaining oxygen incorporates into the AlN grains through the following reaction:

$$Al_2O_3 \xrightarrow{3AlN} 2Al_{Al}^{\times} + 3O_N^{\bullet} + V_{Al}''' \quad (1)$$

The oxygen defects, substituting for a nitrogen ion and consequently produced aluminum vacancies, are believed to limit the electrical and thermal conductivity [11–18]. Jang and Choi [12,13] propose that the aluminum vacancies are the charge carrier for the AlN ceramics. Similar conclusions were also drawn from the DC polarization and impedance spectroscopy experiment, suggesting that ionic conduction of AlN grains was more dominant than electronic conduction, with grain boundary blocking effects [14].

On the other hand, a carbothermal reduction has been studied to produce AlN powder of a high quality from aluminum hydroxide or oxide [19–21]. The carbothermal reduction is expressed as follows:

$$Al_2O_3 + 3C + N_2 \rightarrow 2AlN + 3CO \quad (2)$$

Here the oxygen in the precursor is removed under a nitrogen atmosphere. The reaction depends on the type of AlN precursor, the reduction atmosphere, and the temperature.

Although both the addition of sintering additives and a carbothermal reduction contribute to the oxygen removal of AlN ceramics, their interrelational effects on electrical and thermal properties have yet to be fully understood. Jackson et al. [6]

* Corresponding author. Tel.: +82 31 645 1441; fax: +82 31 645 1492.
E-mail address: smlee@kicet.re.kr (S.-m. Lee).

0272-8842/$36.00
doi:10.1016/j.ceramint.2010.04.001

studied the effects of amounts of Y_2O_3 sintering additive on the thermal conductivity of AlN ceramics extensively; however, they did not observe the electrical properties. Various studies of the preparation of AlN powder through carbothermal reduction can be found in the literature [19–21]. However, the effects of a carbothermal reduction on both the electrical and thermal conductivities of AlN ceramics have not been elucidated. In this study, the effect of the amount of sintering additive and the carbothermal reduction during sintering on both the electrical and thermal properties of AlN ceramics are investigated. To do this, carbon was added to aluminum nitride ceramics with different amounts of Y_2O_3 sintering additives. The electrical properties of the DC volume resistivity were measured, and the grain and grain boundary resistivities were resolved using impedance spectroscopy. They were then compared with the thermal conductivities, to understand the effects of carbothermal reduction on the role of ionic defects on their interrelationship.

2. Experimental procedure

A commercial AlN powder (E-grade, Tokuyama Soda, Tokyo, Japan) with an average size of 1 μm and surface area of 3 m^2/g was used. According to the manufacturer data, the powder's major impurity consisted of 0.85 wt% oxygen. As sintering aids, 3, 5, and 10 wt% of Y_2O_3 (grade C, 0.3 μm, H.C., Starck, Germany) were mixed with the AlN powder. For the carbothermal reduction, an additional 0.5 wt% carbon powder (Corax N774, Evonik Carbon Black Korea Co., Ltd., Korea) with an average size of 60 nm and surface area of 29 m^2/g was introduced to the powder batches. The proportioned powder mixtures were ball-milled with an anhydrous ethyl alcohol medium in Teflon jars for 20 h. The prepared slurry was dried in an oven 70 °C for 24 h and then hot-pressed in a graphite furnace at 1750 °C for 3 h under an applied pressure of 20 MPa in a nitrogen atmosphere. For carbon-added specimens, carbothermal reductions were conducted at 1400 °C for 5 h while heating to isothermal holding at 1750 °C.

The DC volume resistivity was measured under an electric field of 250 V/mm after a charging time of 60 s. Impedance spectroscopy analysis was applied between 200 and 400 °C using a frequency response analyzer (SI-1260, Solartron Analytical, UK) with a high impedance adapter (SI-1296, Solartron Analytical, UK). For these measurements, the specimens were first sliced into a disk 1 mm in thickness and both surfaces were then ground using #2000 SiC paper. After grinding, silver paste was applied as the electrodes and this was annealed at 850 °C for 30 min. The measured impedance spectrum was fitted to semicircles using Zview software (ver. 3.0, Scribner, Germany). The thermal diffusivity was measured using the laser-flash method (LFA427, Netzsch, Germany), and the thermal conductivity was calculated using the heat capacity of pure AlN [22] and the measured density of the AlN ceramics prepared in this study.

For the observation of the microstructure, the specimens were polished up to 3 μm using diamond paste and then using 1 and 0.3 μm alumina suspensions. Structures and chemistry of grain boundaries were analyzed using transmission electron microscopy (JEM4010, JEOL, Tokyo, Japan) with beam probe size of around 10 nm. For oxygen content analysis, electron probe microanalysis technique was used (JXA-8100, JEOL, Tokyo, Japan). A few specimens were exposed to fluorine plasma produced by a typical inductively coupled plasma etcher (Versaline, Unaxis Co., USA). The surface microstructures were then observed using a scanning electron microscope. The plasma exposure time was 60 min. The details of the test conditions are given in Table 1.

Table 1
Plasma etch condition for AlN ceramics.

Parameters	Condition
RF power (W)	700
RF power (bias)	200
(bias voltage)	(334)
CF_4 (SCCM)	30
O_2 (SCCM)	5
Ar (SCCM)	10
Pressure (mTorr)	10

3. Results and discussion

Fig. 1 shows crystalline phase developments with or without a carbothermal reduction. A carbon addition and carbothermal

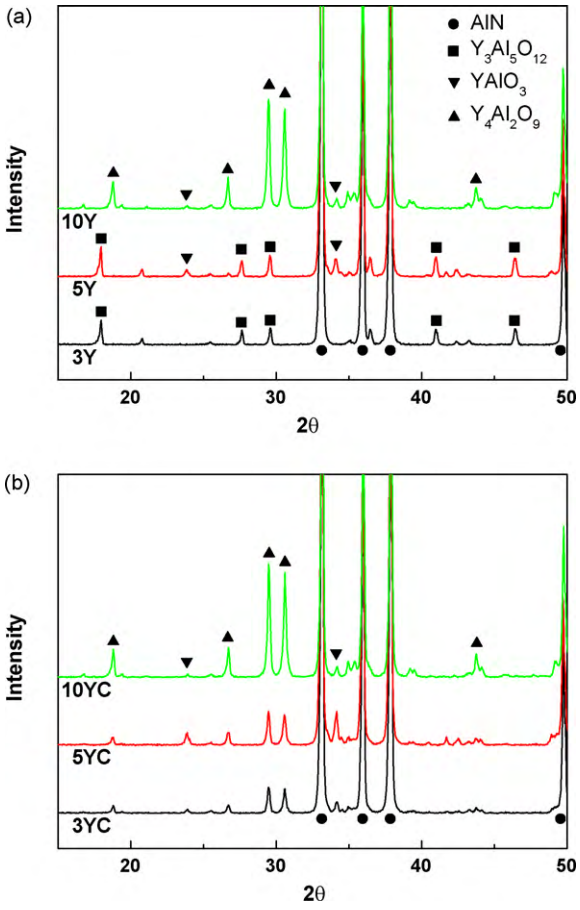

Fig. 1. XRD patterns of the specimens sintered at 1750 °C for 3 h: (a) without and (b) with a carbothermal reduction.

Table 2
Crystalline phases with or without carbothermal reduction.

Code	Additives	Crystalline phases
3Y	3 wt% Y_2O_3	$Y_3Al_5O_{12}$
5Y	5 wt% Y_2O_3	$Y_3Al_5O_{12}/YAlO_3$
10Y	10 wt% Y_2O_3	$Y_4Al_2O_9/YAlO_3$
3YC	3 wt% Y_2O_3, 0.5 wt% C	$Y_4Al_2O_9/YAlO_3$
5YC	5 wt% Y_2O_3, 0.5 wt% C	$Y_4Al_2O_9/YAlO_3$
10YC	10 wt% Y_2O_3, 0.5 wt% C	$Y_4Al_2O_9/YAlO_3$

reduction resulted in the development of yttrium-rich second phases (Table 2). For instance, in the 5Y specimen, the second phases moved from the $Y_3Al_5O_{12}/YAlO_3$ to the $YAlO_3/Y_4Al_2O_9$ region, implying that oxygen was removed by the carbothermal reduction. However, the observed phase developments showed that the oxygen content of the sintered body without a carbothermal reduction is higher than that expected from AlN starting powder and a sintering additive. This may be due to the oxygen that was taken during the powder processing. Indeed, when total oxygen contents were measured for 5Y and 5YC specimens, we found that they are 2.6 and 2.1 wt%, respectively, which means that additional oxygen was taken during powder processing and some of them was removed by the carbothermal reduction. In contrast to the 3Y and 5Y specimens, the 10Y specimen did not show the movement of the second phase field by the carbothermal reduction.

Fig. 2 shows the temperature dependencies of the DC volume resistivities measured after 60 s in an electric field of 250 V/mm. The carbothermal reduction resulted in 2 or 3 orders of magnitude higher resistivities in 3YC and 5YC than in the 3Y and 5Y specimens, accompanying the changes in the second phase. However, the 10Y specimens did not show such a change in DC volume resistivity after a carbothermal reduction. Those changes in resistivities were not caused by their grain size or grain boundary area effects, since all the specimens showed nearly the same grain size. Instead, the DC volume resistivity may be related to the phase developments of yttrium-aluminates. This is supported by the fact that the 10Y and 5YC

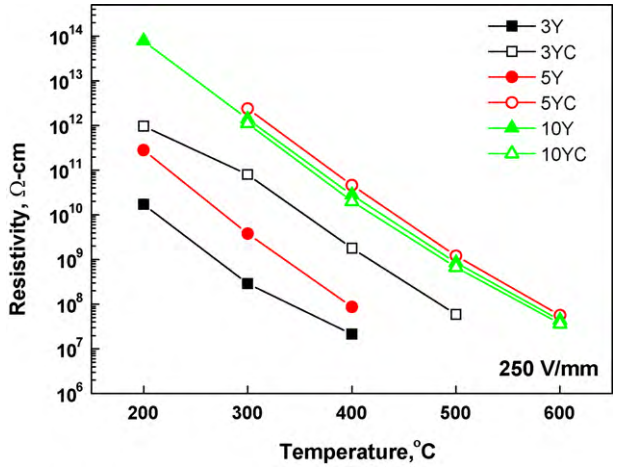

Fig. 2. Volume resistivities with respect to temperatures for the specimens with various amounts of Y_2O_3 additives with or without a carbothermal reduction.

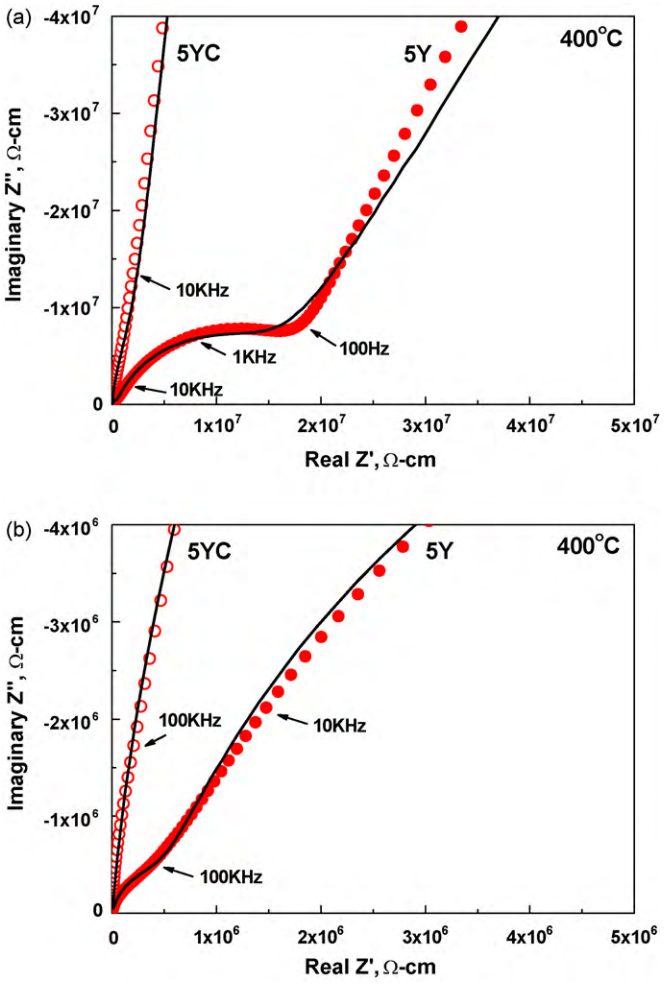

Fig. 3. Complex impedance spectrum of 5Y and 5YC specimens: (a) lower frequency and (b) higher frequency region (solid lines are fitted curves).

specimens showed similar DC resistivities even when the $YAlO_3/Y_4Al_2O_9$ ratios were different for two specimens.

To understand the behaviors of the DC volume resistivity, an AC impedance analysis was conducted with the 5Y and 5YC specimens (Fig. 3). Without a carbon addition, the impedance spectra showed two circles. The lower resistivity component in a higher frequency region of the impedance spectrum of the 5Y specimen showed nearly a semicircle, indicating a narrow distribution of the relaxation times (Fig. 3(b)). The dielectric constant was calculated to be approximately 12, showing that the semicircle came from the AlN grains. Thus, the intercept of the semicircle must be related to ionic conduction of AlN grains similar to the previous study [12–14].

On the other hand, the higher resistivity component in the lower frequency region (Fig. 3(a)) showed an enlarged and depressed semicircle, indicating significantly increased grain boundary resistance and a wide distribution of the relaxation times of diverse grain boundaries. In contrast to the 5Y specimen, the 5YC specimen showed significantly increased grain boundary resistivity, though it was not easy to deconvolute the two semicircles due to grains and grain boundaries.

Fig. 4 shows summaries of the resistivities of the grain and grain boundaries with or without carbothermal reduction as a

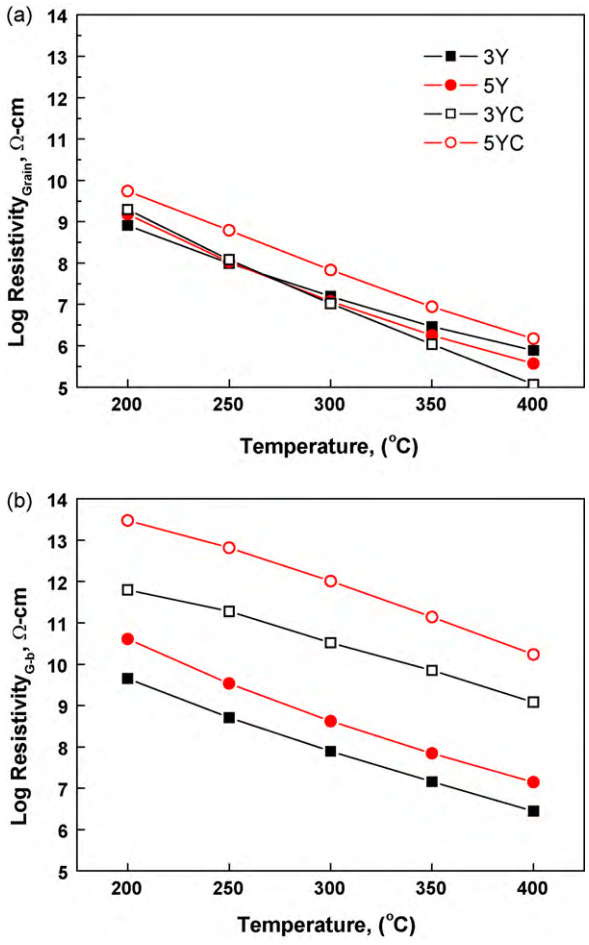

Fig. 4. (a) Fitted grain and (b) grain boundary resistivities for 3Y, 5Y, 3YC and 5YC specimens.

function of the temperature. Although the grain resistivities varied moderately, at less than 1 order of magnitude depending on the Y_2O_3 content and on whether carbothermal reduction was utilized, the grain boundary resistivities changed significantly, which is consistent with the DC volume resistivity changes of 2 or 3 orders of magnitude.

Thermal conductivities depended on the Y_2O_3 content and on the carbothermal reduction (Fig. 5). As Y_2O_3 increased from 3 to 5 wt%, the thermal conductivity increased and then slightly decreased with the 10Y specimen, as in the results found in the literature [6]. For the 3Y specimen, the application of carbothermal reduction resulted in an increase in the thermal conductivity that was equivalent to a Y_2O_3 content of 5 wt%. If it is considered that oxygen substitution and consequent aluminum vacancies have significant effects on the thermal conductivity, the addition of carbon and a carbothermal reduction in the 3Y specimen must be a result of oxygen removal during the carbothermal reduction. However, a further increase in the thermal conductivity appears to be limited due to the relatively low sintering temperature of 1750 °C, used in this study.

From comparisons of several electrical resistivities of the grain, grain boundary and DC resistivity with thermal conductivities, the thermal conductivity appears to be more relevant to the grain resistivity. As is well known from early

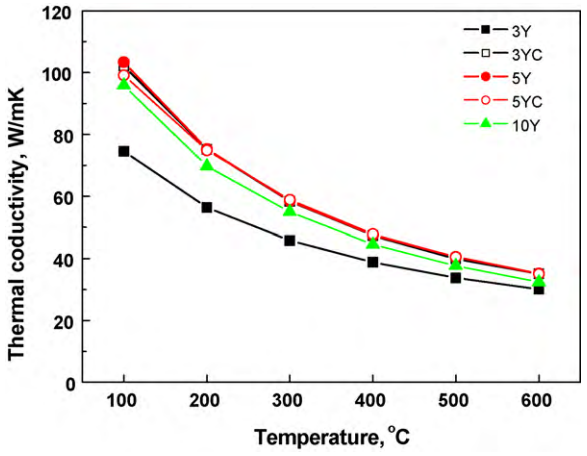

Fig. 5. Thermal conductivities of various specimens with or without a carbothermal reduction.

works [6,11], thermal conductivity is a function of the concentration of lattice defects, such as those caused by aluminum vacancies. The concentrations are related to the thermal conductivity, following the equation:

$$\frac{\Delta n}{n_0} \approx \frac{1}{\alpha}\left(\frac{1}{k} - \frac{1}{k_0}\right), \tag{3}$$

where k_0 is the thermal conductivity of pure AlN, at 320 W/mK, n_0 is density of N atoms, Δn is the lattice defect density, and α is a proportional constant of 0.43 mK/W. On the other hand, ionic conductivity is expressed with respect to mobile ionic defects following:

$$\sigma = 3e\mu n_{\text{defect}}, \tag{4}$$

where μ is the mobility and n_{defect} is the density of the ionic charge carriers of aluminum vacancies. For instance, for the 3Y and 3YC specimens, $\Delta n/n_0$ is 0.057 and 0.039, respectively. The difference in this case is less than a factor of 2. The difference in the defect concentration can affect the electrical conductivities in several ways. From the various resistivities shown in Figs. 3 and 4, only the resistivity of the grains varied within several factors after a carbothermal reduction, implying that the grain resistivity is more relevant to the thermal conductivity. In terms of the grain boundary resistivity, it changed by 2 or 3 orders of magnitude after a carbothermal reduction in 3 or 5 wt% Y_2O_3-added specimens. The DC volume resistivity at a high electrical field also showed significant variation after a carbothermal reduction. Thus, only the grain resistivity and thermal conductivity of the ceramics appear to be correlated. This seems feasible considering that the grain boundaries affecting the electrical conduction generally have thicknesses of around several nanometers, which are much narrower than the thicknesses of grains.

To understand this grain boundary behavior, we checked structure and chemistry of grain boundaries. Fig. 6 shows that the grain boundaries seem to be free of glassy film, which can be expected from our sintering temperature far below the liquid formation temperature ~1850 °C between Y_2O_3 and Al_2O_3. In the grain boundary regions yttrium enrichment was observed

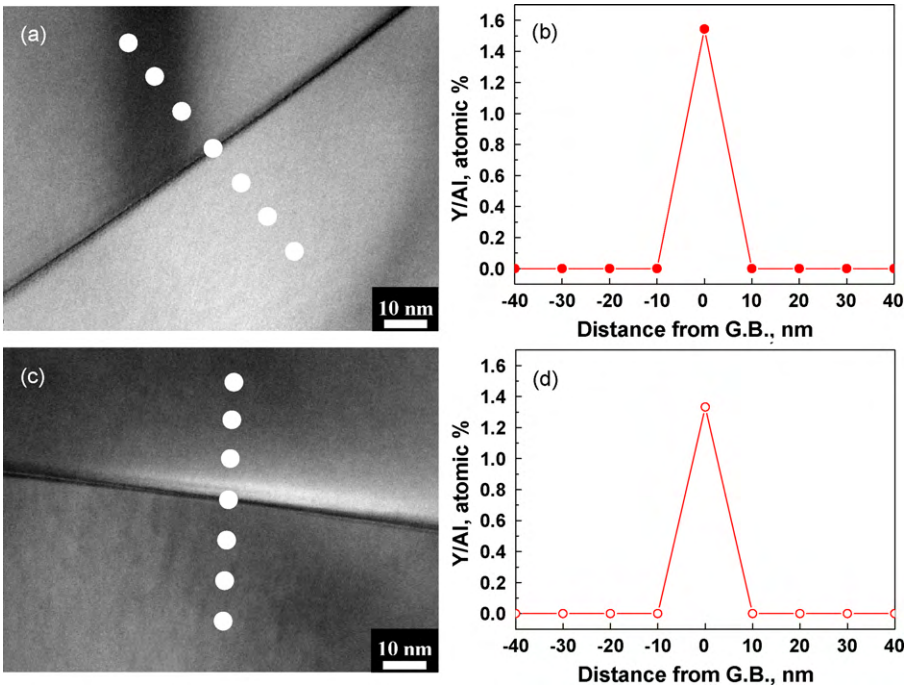

Fig. 6. TEM microstructures and EDX analysis of the grain boundary region: (a and b) 5Y and (c and d) 5YC.

regardless of carbothermal reduction, implying that yttrium segregated in the grain boundary. The thickness of the segregated region appeared less than 10 nm. This enrichment of yttrium must affect the charge transport through grain boundary, but the details of the mechanism and effects of carbothermal reduction are still under investigation.

Fig. 7 shows backscattered electron images of the polished specimens. The white phases are yttrium-aluminate second phases. While increases in the Y_2O_3 content produce more second phases (Fig. 6(a) and (c)), carbothermal reductions resulted in fewer second phases (Fig. 6(b) and (d)). When the image was processed digitally, the area fraction of the white

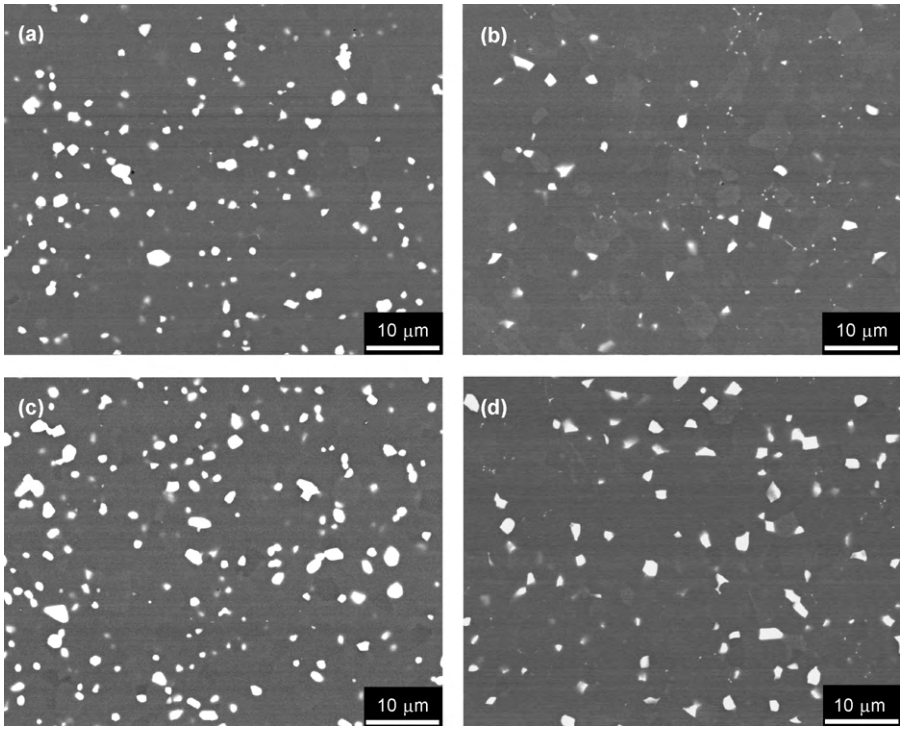

Fig. 7. SEM microstructures of specimens: (a) 3Y, (b) 3YC, (c) 5Y, and (d) 5YC.

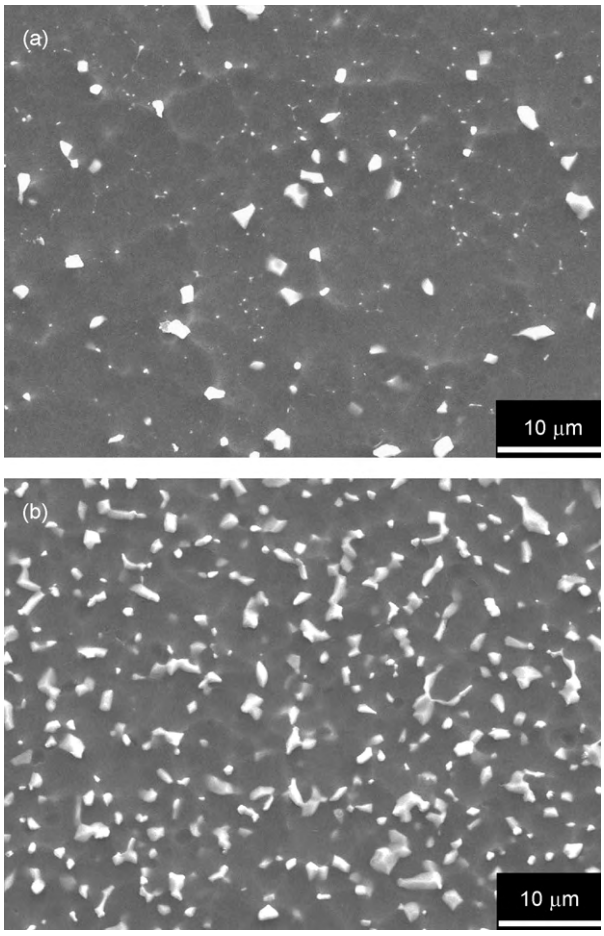

Fig. 8. Surface microstructures of (a) 5YC and (b) 10Y after fluorine plasma exposure for 60 min.

region was reduced from 4.9 and 8.8% to 2.6 and 5.8% via a carbothermal reduction for the 3Y and 5Y specimens, respectively. The decreases in the amount of the second phases must have been caused by oxygen removal and hence reduced aluminum oxide by a carbothermal reduction during sintering.

The reduced amounts of second phases by the carbothermal reduction may contribute to the plasma resistances of AlN ceramics, as higher plasma resistance implies a lower tendency of contamination particles. When the 5YC and 10Y specimens were etched under the same fluorine plasma, they showed completely different microstructures after a plasma exposure (Fig. 8). The AlN matrix eroded faster than the yttrium-aluminate second phases, resulting in protruding particles on the surface. The protruding particles were expected to detach after prolonged exposure, resulting in the generation of the contamination particles. Therefore, although the electrical and thermal properties of the 5YC and 10Y specimens were similar, the expected plasma resistance, that is, a tendency toward lower particle generation, must be higher in the 5YC specimen.

4. Conclusions

This study investigated the effects of a carbothermal reduction on the thermal and electrical properties of AlN ceramics. Carbothermal reduction resulted in significantly increased DC electrical resistivities whose effects were pronounced for 3 or 5 wt% Y_2O_3-added specimens. When these specimens were analyzed using an impedance spectroscopy technique, the grain boundary resistivity was found to increase significantly, which was in contrast to the moderate changes in the grain resistivities after a carbothermal reduction. These resistivity changes were accompanied by second phase developments. From a comparison between the thermal and several electrical conductivities, the thermal properties appeared more relevant to the resistivities of AlN grains. Thermal conductivity was enhanced by the carbothermal reduction of 3 wt% Y_2O_3-added specimens but was not distinct in specimens with a higher Y_2O_3 content. In addition, we found an yttrium enrichment in the grain boundary region.

References

[1] D.R. Wright, L. Chen, P. Federlin, K. Forbes, Manufacturing issues of electrostatic chucks, J. Vac. Sci. Technol. B 13 (1995) 1910–1916.
[2] J.F. Daviet, I. Peccoud, Electrostatic clamping applied to semiconductor plasma processing-I. Theoretical modeling, J. Electrochem. Soc. 140 (1993) 3245–3256.
[3] R. Atkinson, A simple theory of the Johnsen–Rahbek effect, Brit. J. Appl. Phys. 2 (1969) 325–332.
[4] G. Kalkowski, S. Risse, G. Harnisch, V. Guyenot, Electrostatic chucks for lithography applications, Microelectron. Eng. 57–58 (2001) 219–222.
[5] T. Watanabe, T. Kitabayashi, C. Nakayama, Electrostatic force and absorption current of alumina electrostatic chuck, Jpn. J. Appl. Phys. 31 (1992) 2145–2150.
[6] T.B. Jackson, A.V. Virkar, K.L. More, R.B. Dinwiddie, R.A. Cutler, High-thermal-conductivity aluminium nitride ceramics: the effect of thermodynamic, kinetic and microstructural factors, J. Am. Ceram. Soc. 80 (1997) 1421–1435.
[7] S.L. Shindé, J.S. Goela, High Thermal Conductivity Materials, Springer, New York, 2006, pp. 143–166.
[8] E. Hagen, Y. Yu, T. Grande, R. Hløier, M.–A. Einarsrud, Sintering of AlN ceramics using CaO-Al_2O_3 as sintering additive—chemistry and microstructural development, J. Am. Ceram. Soc. 85 (2002) 2971–2976.
[9] L. Qiao, H. Zhou, H. Xue, S. Wang, Effect of Y_2O_3 on low temperature sintering and thermal conductivity of AlN ceramics, J. Eur. Ceram. Soc. 23 (2003) 61–67.
[10] W.J. Kim, D.K. Kim, C.H. Kim, Morphological effect of second phase on the thermal conductivity of AlN ceramics, J. Am. Ceram. Soc. 79 (1996) 1066–1072.
[11] G.A. Slack, R.A. Tanzill, P.O. Pohl, J.W. Vandersande, The intrinsic thermal conductivity of AlN, J. Phys. Chem. Solids 48 (1987) 641–647.
[12] S.A. Jang, G.M. Choi, Effects of dopants on the complex impedance and dielectric properties of aluminum nitride, J. Am. Ceram. Soc. 75 (1992) 3145–3148.
[13] S.A. Jang, G.M. Choi, Electrical conduction in aluminum nitride, J. Am. Ceram. Soc. 76 (1993) 957–960.
[14] W.J. Lee, S.M. Lee, K.B. Shim, H.T. Kim, Effects of sintering conductions on the electrical conductivity of 1 wt% Y_2O_3-doped AlN ceramics, J. Korean Ceram. Soc. 44 (2007) 116–123.
[15] M. Yahagi, K.S. Goto, Ionic conductivity of AlN containing Y_2O_3 or Al_2O_3 at 1173–1773, J. Jpn. Inst. Met. 47 (1983) 419–425.
[16] H. Nakanto, K. Watari, H. Hayashi, K. Urabe, Microstructural characterization of high-thermal-conductivity aluminum nitride ceramic, J. Am. Ceram. Soc. 85 (2002) 3093–3095.

[17] W.A. Groen, P.F. van Hal, High temperature electrical conductivity of AlN ceramics, Brit. Ceram. Trans. 93 (1994) 192–195.
[18] R.W. Francis, W.L. Worrel, High temperature electrical conductivity of aluminum nitride, J. Electrochem. Soc. 123 (1976) 430–433.
[19] H.U. Joo, W.S. Jung, Effects of carbon monoxide of the carbothermal reduction and nitridation reaction of alumina, J. Mater. Process. Technol. 204 (2008) 498–501.
[20][19] S. Xi, X. Liu, P. Li, J. Zhou, AlN ceramics synthesized by carbothermal reduction of mechanical activated Al_2O_3, J. Alloys Compd. 457 (2008) 452–456.
[21] M. Halmann, A. Frei, A. Steinfeld, Carbothermal reduction of alumina: thermochemical equilibrium calculations and experimental investigation, Energy 32 (2007) 2420–2427.
[22] J.F. Shackelford, CRC Materials Science and Engineering Handbook, third ed., 2001, p. 378.